

General Relativistic Simulations of Jet Formation by a Rapidly Rotating Black Hole

Shinji Koide

Faculty of Engineering, Toyama University,
Gofuku 3190, Toyama 930-8555,
Japan.

David L. Meier

Jet Propulsion Laboratory,
4800 Oak Grove Dr. Pasadena, CA 91109,
USA.

Kazunari Shibata*, Takahiro Kudoh
National Astronomical Observatory,
Mitaka, Tokyo 181-8588,
Japan.

September 17, 2018

Abstract

Recent observations of Galactic Black Hole Candidates (BHCs) suggest that those that are superluminal jet sources have more rapid black hole spin rates than otherwise normal BHCs. This provides observational support for models of relativistic jet formation that extract rotational energy of the central black hole. To investigate this mechanism, we have developed a new general relativistic magnetohydrodynamic code in Kerr geometry. Here we report on the first numerical simulation of the formation of a relativistic jet in a rapidly-rotating ($a = 0.95$) Kerr black hole magnetosphere. We assume that the initial velocity of the disk is zero. We find that the maximum velocity of the jet reaches $0.93c$ (Lorentz factor, 2.7) and the terminal velocity of the jet is $0.85c$ (Lorentz factor, 1.9). On the other hand, for a non-rotating ($a = 0$) Schwarzschild black hole, the maximum jet velocity is less than $0.6c$ as far as we calculated with the similar condition of the magnetosphere to that of the Kerr black hole case. These numerical results show the importance of the rapidly rotating black hole for the relativistic jet formation clearly.

1 Introduction

Radio jets ejected from radio loud active galactic nuclei (AGNs) sometimes show proper motion with apparent velocity exceeding the speed of light c [1, 2]. The widely-accepted explanation for this phenomenon, called superluminal motion, is relativistic jet flow in a direction nearly along the observer's line-of-sight with a Lorentz factor greater than 2.0 [3]. Such relativistic motion is thought to originate from a region very close to the putative supermassive black hole which is thought to power each AGN [4, 5]. On the other hand, the great majority of AGN are

*Present address: Hanayama Observatory, Kyoto University, Kita-Hanayama, Yamashina-ku, Kyoto, 607-8471, Japan.

radio quiet and do not produce powerful relativistic radio jets [5]. These two classes of active objects (radio loud and quiet) are also found in the black hole candidates (BHCs) in our own Galaxy. Objects with superluminal jets, such as GRS 1915+105 and GRO J1655-40, belong to the radio loud class [6, 7]. Other objects such as Cyg X-1 and GS 1124-68 are relatively radio quiet and produce little or no jet.

What causes the difference between the two classes? Recent observations of the BHCs in our Galaxy suggest that the Galactic superluminal sources contain very rapidly rotating black holes (specific angular momentum of rotating black hole $a = 0.9 - 0.95$), while the black holes in Cyg X-1 and GS 1124-68 are spinning much less rapidly ($a = 0.3 - 0.5$) [8]. According to recent (nonrelativistic) studies of magnetically-driven jets from the accretion disk by Kudoh & Shibata [9, 10], the terminal velocity of the formed jet is comparable to the rotational velocity of the disk at the foot of the jet. Further nonrelativistic simulations of jet formation confirm these results [11, 12], except for the extremely large magnetic field case [13] in which very fast jets can be produced. The rotation velocity at the innermost stable orbit of the Schwarzschild black hole ($r = 3r_S$) is $0.5c$. (Here $r_S = 2GM_{\text{BH}}/c^2$ is the Schwarzschild radius, where G and M_{BH} are the gravitational constant and black hole mass, respectively.) In addition, recent studies indicate that the poloidal magnetic field strengths in disks around non-rotating black holes may be rather weak [14]. Therefore, a jet produced by MHD acceleration from an accretion disk around a non-rotating black hole should be sub-relativistic and very weak. In fact, numerical simulations of jet formation in a Schwarzschild metric show only sub-relativistic jet flow [15], except for the case with the artificial condition of a hydrostatic corona in equilibrium [16].

Several mechanisms for relativistic jet formation from rotating black holes have been proposed [17, 18, 19, 20]. However, up until now no one has performed a self-consistent numerical simulation of the dynamic process of jet formation in a rotating black hole magnetosphere. To this end, we have developed a Kerr general relativistic magnetohydrodynamic (KGRMHD) code. In this paper we report briefly on what we believe is the first calculation of its kind — simulation of relativistic jet formation in a rotating black hole magnetosphere. When the rotation parameter of the rotating black hole $a = 0.95$, the maximum velocity of the formed jet reaches $0.93c$ (Lorentz factor, $\gamma = 2.7$), and the terminal velocity is $0.85c$ ($\gamma = 1.9$). On the other hand, when a vanishes, only a slow jet is formed even if the initial condition of magnetosphere is almost the same as that of the Kerr black hole case. This result clearly shows the importance of the rapidly spinning black hole for the formation of relativistic jet.

2 Numerical Method

We use a $3 + 1$ formalism of the general relativistic conservation laws of particle number, momentum, and energy and Maxwell equations with infinite electric conductivity [21]. The Kerr metric, which provides the spacetime around a rotating black hole, is used in the calculation. When we use Boyer-Lindquist coordinates, $x^0 = ct$, $x^1 = r$, $x^2 = \theta$, and $x^3 = \phi$, the Kerr metric $g_{\mu\nu}$ is written as follows,

$$ds^2 = g_{\mu\nu}dx^\mu dx^\nu = -h_0^2(cdt)^2 + \sum_{i=1}^3 h_i^2(dx^i)^2 - 2h_3\Omega_3 cdt dx^3. \quad (1)$$

By modifying the lapse function in our Schwarzschild black hole code ($\alpha = \sqrt{1 - r_S/r}$) to be $\alpha = \sqrt{h_0^2 + \Omega_3^2}$, and adding some terms to Ω_3 , we were able to develop a KGRMHD code relatively easily. (See Appendix C in [15] for more details on this procedure and the meaning of symbols used.)

We use the Zero Angular Momentum Observer (ZAMO) system for the 3-vector quantities, such as velocity \mathbf{v} , magnetic field \mathbf{B} , and so on. For scalars, we use the frame comoving with the fluid flow. The simulation of the Kerr (Schwarzschild) black hole is performed in the region $0.75r_S$ ($1.2r_S$) $\leq r \leq 20r_S$, $0 \leq \theta \leq \pi/2$ with 210×70 mesh points, assuming axisymmetry with respect to the z -axis and mirror symmetry with respect to the plane $z = 0$. A simplified radiative boundary condition is employed at $r = 0.75r_S$ ($r = 1.2r_S$) and $r = 20r_S$ for the Kerr (Schwarzschild) black hole case. In the simulations, we use simplified tortoise coordinates,

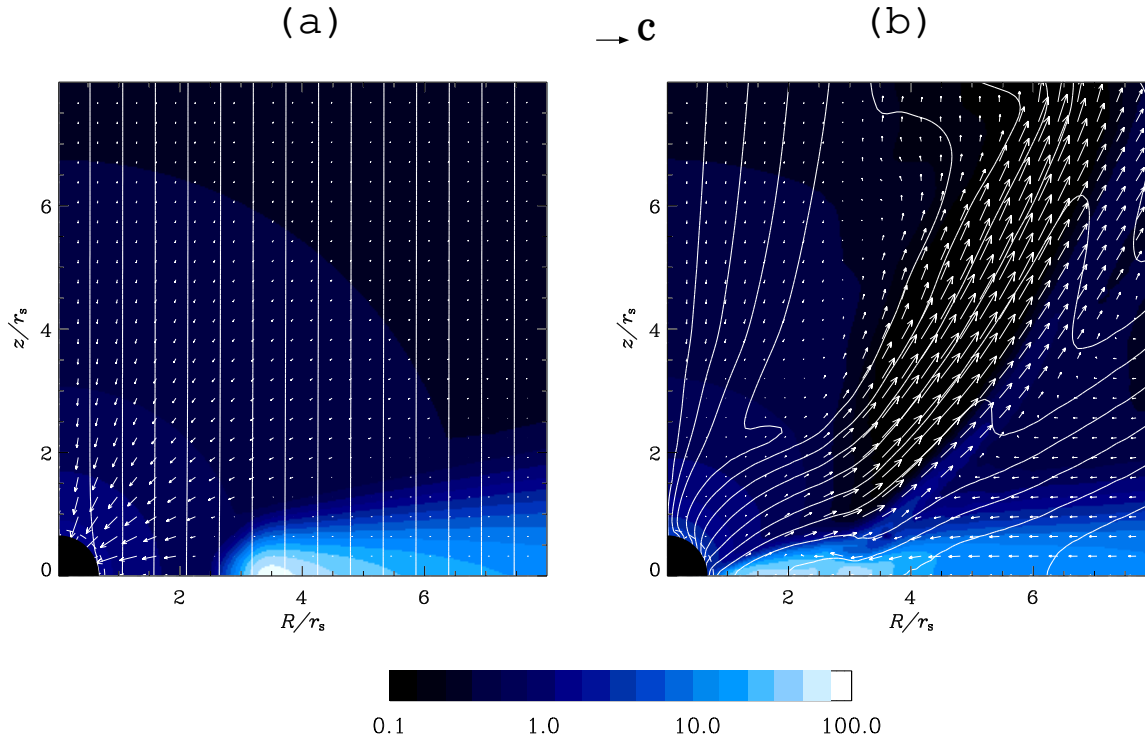


Figure 1: A relativistic jet formation around a Kerr black hole (rotation parameter $a = 0.95$). (a) Initial. (b) Final stage at $t = 65\tau_S$. Color shows the logarithm of mass density. Vector indicates the velocity. The lines show the magnetic field. The broken line near the horizon shows the inner boundary of the calculation region. The relativistic jet are formed at $t = 65\tau_S$. The maximum velocity of the jet is $0.93c$ (Lorentz factor, $\gamma = 2.7$) and the terminal velocity is $0.85c$ ($\gamma = 1.9$). The solid straight line shows the plot line used in Fig. 3.

$x = \log(r/r_H - 1)$, where r_H is the radius of the black hole horizon. Here $r_H = 0.656r_S$ ($r_H = r_S$) when $a = 0.95$ ($a = 0$). To avoid numerical oscillations, we use a simplified TVD method [15, 22, 23, 24]. We checked the KGRMHD code by computing Keplerian motion around a rotating black hole and comparing with analytic results.

3 Results

Figure 1 shows the initial and final states of the calculation of relativistic jet formation near a Kerr black hole. These figures show the rest mass density (color), velocity (vector), and magnetic field (solid lines) in $0 \leq R \leq 8r_S$, $0 \leq z \leq 8r_S$. The poloidal magnetic field lines are drawn as the contour lines of the azimuthal (ϕ) component of the four vector potential ($A_t, A_r, A_\theta, A_\phi$). The black region at the origin shows the black hole horizon. The specific angular momentum of the black hole is $a = 0.95$ and the radius is $r_H = 0.656r_S$. The initial state in the simulation consists of a hot corona and a cold accretion disk around the black hole (Fig. 1a). In the corona, plasma are assumed to be nearly stationary falling with the specific enthalpy $h/\rho c^2 = 1 + \Gamma p/[(\Gamma - 1)\rho c^2] = 1.3$, where ρ is the rest mass density, p is the pressure, and Γ is specific heat ratio and set $\Gamma = 5/3$. Far from the hole, it becomes the stationary transonic solution exactly. The accretion disk is located at $|\cot\theta| \leq 0.125$, $r \geq r_D = 3r_S$ and the initial velocity of the disk is assumed to be zero. The mass density of the disk is 300 times that of the corona. In addition, the magnetic field crosses the accretion disk perpendicularly. We use the vector potential A_ϕ of the Wald [25] solution to set the magnetic field, which

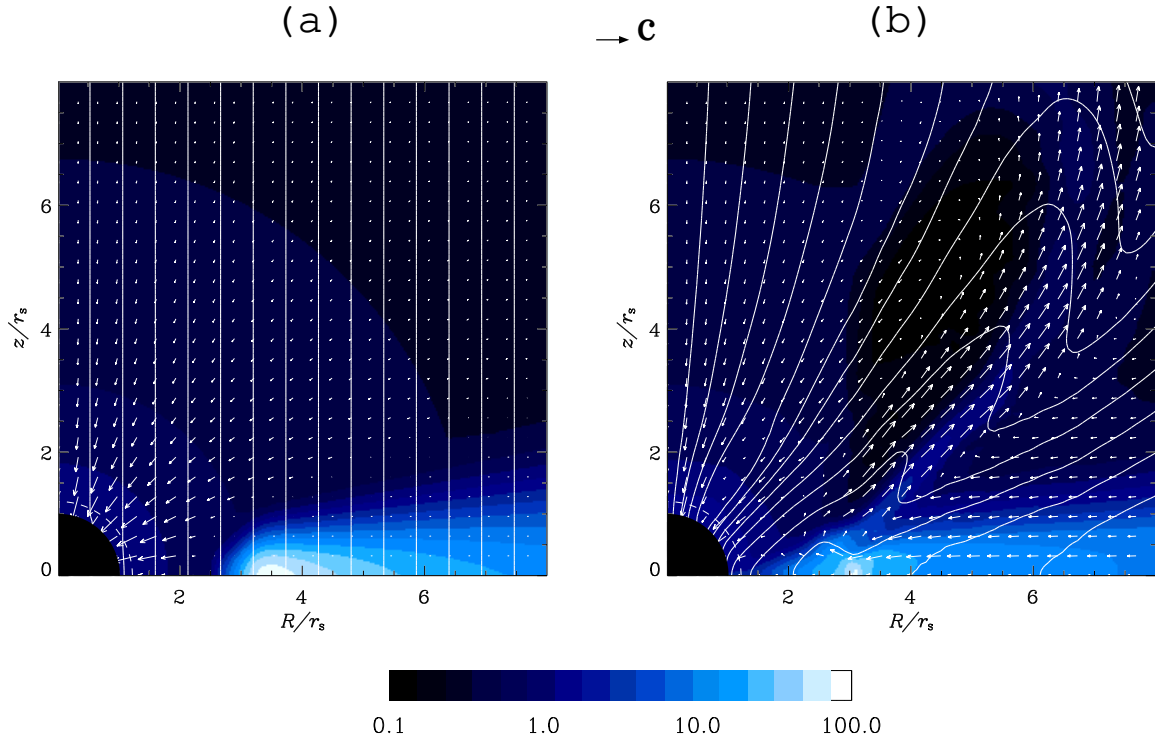


Figure 2: A sub-relativistic jet formation around Schwarzschild black hole ($a = 0$). (a) Initial (b) Final stage at $t = 65\tau_S$. Color shows the logarithm of mass density. Vector indicates the velocity. The lines show the magnetic field. The broken line near the horizon shows the inner boundary of the calculation region. The maximum and terminal velocities of the jet are $0.6c$ and $0.45c$, both sub-relativistic, respectively. The solid straight line shows the plot line used in Fig. 4.

produces a uniform magnetic field far from the Kerr black hole. However, we do not use A_t from the Wald solution; instead, we use the ideal MHD condition $\mathbf{E} + \mathbf{v} \times \mathbf{B} = 0$ to determine the electric field \mathbf{E} . Here the Alfvén velocity and plasma beta value at the disk ($r = 3r_S$) are $v_A = 0.01c$ and $\beta \sim 12$, respectively.

Figure 1b shows the state at $t = 65\tau_S$, where τ_S is defined as $\tau_S \equiv r_S/c$. The accretion disk falls into the black hole rapidly, and the disk plasma crosses the horizon, as suggested by the crowded magnetic field lines near the horizon. The magnetic field lines become radial due to the dragging by the disk near the black hole. The jet is formed almost along the magnetic field lines, while outside of the jet, the magnetic field lines are bent strongly. The maximum velocity of the jet reaches to $0.93c$ (Lorentz factor, $\gamma = 2.7$) at $R = 5.3r_S$, $z = 4.4r_S$ and its terminal velocity is $0.85c$ ($\gamma = 1.9$). The terminal velocity is defined by the jet velocity far from the black hole ($r \sim 10r_S$). We found the jet has a two-layered-shell structure with respect to the density. The low density part of the jet is fast and relativistic, while the high density part at the outer shell is slower and sub-relativistic. The fast jet dominates the jet and the slow, dense jet is thin. The high density jet is connected to the high density region of the accretion disk.

To show the importance of the black hole rotation for relativistic jet formation, we also performed a simulation of the Schwarzschild black hole case ($a = 0$) (see Fig. 2). The initial condition is almost the same as that of Kerr black hole case except for the black hole rotation (Fig. 2a). In the initial stage, the coronal plasma is assumed to be stationary falling with $h/\rho c^2 = 1.3$ (see Fig. 2a). The disk is located at the same place of the Kerr black hole case: $|\cot\theta| \leq 0.125$, $r \geq r_D = 3r_S$, and the density of the disk is also 300 times larger than that of corona. The uniform magnetic field crosses the disk perpendicularly. The strength is the same as that of the Kerr case. Figure 2b shows the state at $t = 65\tau_S$. The maximum velocity of the

jet is $0.6c$ and the jet terminal velocity is $0.45c$, both sub-relativistic. The jet also has two-layered-shell structure. The inner shell has low density, while the outer shell has high density. The high density jet dominates the jet, which is different from the Kerr black hole case. The disk plasma also falls and crosses the event horizon rapidly as the Kerr black hole case. Note that the inner edge of the high density region is not identical with that of disk plasma. The plasma of the disk passes through the edge and falls into the black hole. The small high pressure region is formed at $R \sim 3r_S$ in the disk. The high pressure is caused by the shock in front of the region. The dense jet is accelerated by the high pressure. This mechanism is the same as that of the case of the Kepler disk around the Schwarzschild black hole [16]. The magnetic field lines are also bent by the jet strongly.

To show the structure of the relativistic jet in the Kerr black hole case, various physical quantities on the line $z = R - 0.4r_S$ ($1.3r_S \leq R \leq 6.3r_S$) are shown in Fig. 3. The line is almost along the fast, low density jet (see straight line in Fig. 1b). Figure 3a shows the magnetic pressure from the toroidal component of the magnetic field, $B_\phi^2/2\mu$ is very large near the black hole ($1.3r_S \leq R \leq 2.5r_S$) where μ is the magnetic permeability of the vacuum. Because initial magnetic field is $B_\phi = 0$, $B_z = 0.15\rho_0 c^2 \sqrt{\mu}$, where ρ_0 is the unit mass density, the field increases to more than 60 times the initial magnetic field. This amplification is caused by the shear of the plasma flow observed by the Boyer-Lindquist frame or local nonrotating frame (LNRF) due to the frame dragging effect of the rotating black hole [26, 27, 28]. This effect is called a *metric-shear-driven MHD dynamo* by Meier [28]. With the assumption that the azimuthal velocity component is zero, general relativistic Faraday law of induction and ideal MHD condition yield,

$$\frac{\partial B_\phi}{\partial t} = f_1 B_r + f_2 B_\theta, \quad (2)$$

where $f_1 = c(h_3/h_1)\partial(\Omega_3/h_3)/\partial r$, and $f_2 = c(h_3/h_2)\partial(\Omega_3/h_3)/\partial\theta$. Note that f_2 is one order smaller than f_1 when $a \sim 1$. The ridge of the f_1 profile is located near the spherical surface, $r = r_S$ and the magnetic pressure has a maximum near the surface. Where does the energy of the amplification of the magnetic field comes from? The energy does not come from the gravitational energy or thermal energy of the disk, because this effect occurs even when the plasmas of the disk and corona are rest and cool. The only other possible energy source is the rotation of the black hole itself. In fact, the increase in the azimuthal magnetic field component depends on the shear of the rotational variable Ω_3 . We conclude that the energy of the amplification of the magnetic field is supplied by the extraction of the rotational energy of the black hole. Note that this mechanism of the extraction of the rotational energy is different from the previous electromagnetic mechanisms [17, 19]. The detail comparison with these models will be presented in our following paper. If there is no disk, the magnetic tension causes the azimuthal motion of the plasma to prevent the dynamo. The heavy disk plays an important role to keep the magnetic energy from the energy of the black hole rotation to produce a relativistic jet. We estimate the power from the electro-magnetic field, $W_{EM} = \mathbf{v} \cdot (\mathbf{E} + \mathbf{J} \times \mathbf{B})$ and the gas pressure, $W_{gp} = -\mathbf{v} \cdot \nabla p$ (Fig. 3c). The power contributions of the electromagnetic field and gas pressure are comparable. The high gas pressure is caused by the shock in the disk at $r \sim 2r_S$. The density and the pressure are small in the fast jet region ($3.5r_S \leq R$), which means that the jet comes from the corona, not the disk. Both the strong magnetic and gas pressures push the low density plasma to become the relativistic jet. Figure 3b shows the azimuthal velocity is small over the whole range. This indicates the jet acceleration is caused by the magnetic and gas pressure rather than the magnetic tension (or centrifugal force). The magnetically driven part of the mechanism is the same as that of Uchida & Shibata [29] and Shibata & Uchida [30]. Punsly & Coroniti (1990) proposed an alternative magnetic force driven mechanism of the relativistic jet formation. They considered the magnetic tension causes the azimuthal velocity to produce the jet due to centrifugal force like the model of non-relativistic jet formation from the accretion disk [31]. Figure 3b shows that in the fast jet region ($4r_S \leq R$), the azimuthal velocity is small but positive ($v_\phi > 0$), which is remnant of the frame dragging by the rotating black hole. In the acceleration region ($R < 4r_S$), on the other hand, the azimuthal velocity is negative, as predicted by Meier [28]. Accretion of this negative angular momentum material ultimately reduces the spin of the black hole and is at least partially responsible for extracting the hole's rotational energy.

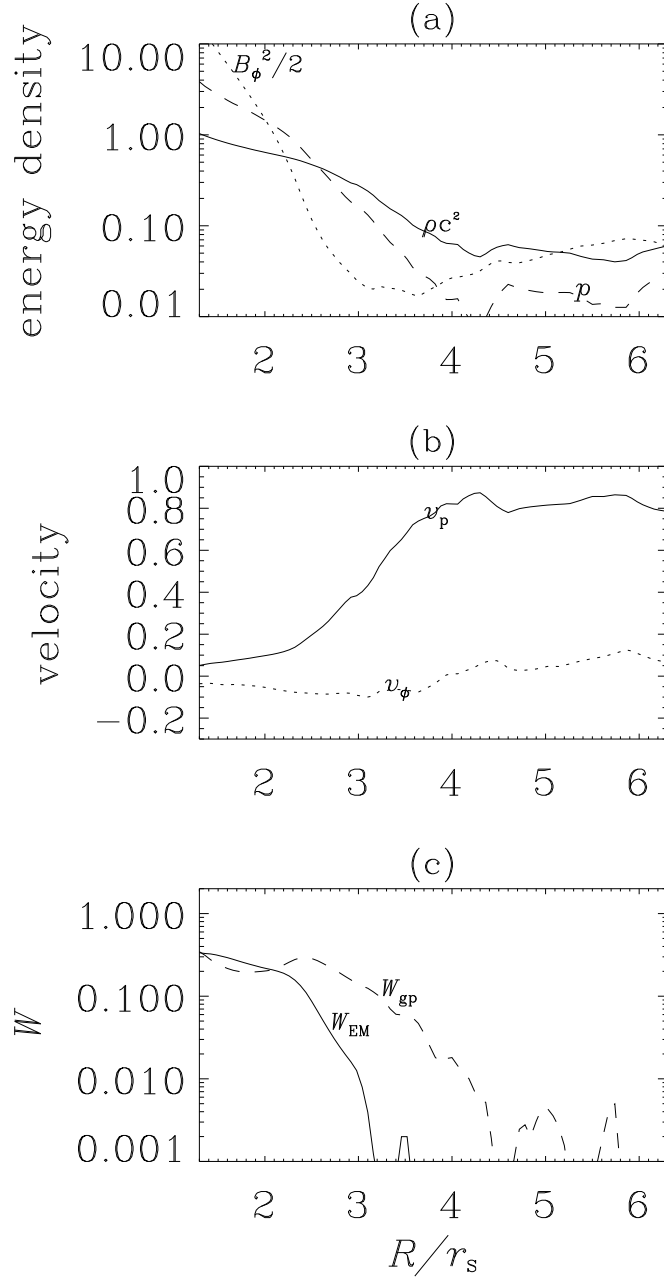


Figure 3: Physical quantities of the Kerr black hole case along $z = R - 0.4r_s$ ($1.3r_s \leq R \leq 6.3r_s$) at $t = 65\tau_S$ (see straight line in Fig. 1b). (a) Mass density, ρ , gas pressure, p , and poloidal magnetic pressure, $B_\phi^2/2$. (b) Poloidal velocity, v_p and azimuthal velocity, v_ϕ . (c) Power of electromagnetic field (W_{EM}) and gas pressure (W_{gp}) to the acceleration of the jet.

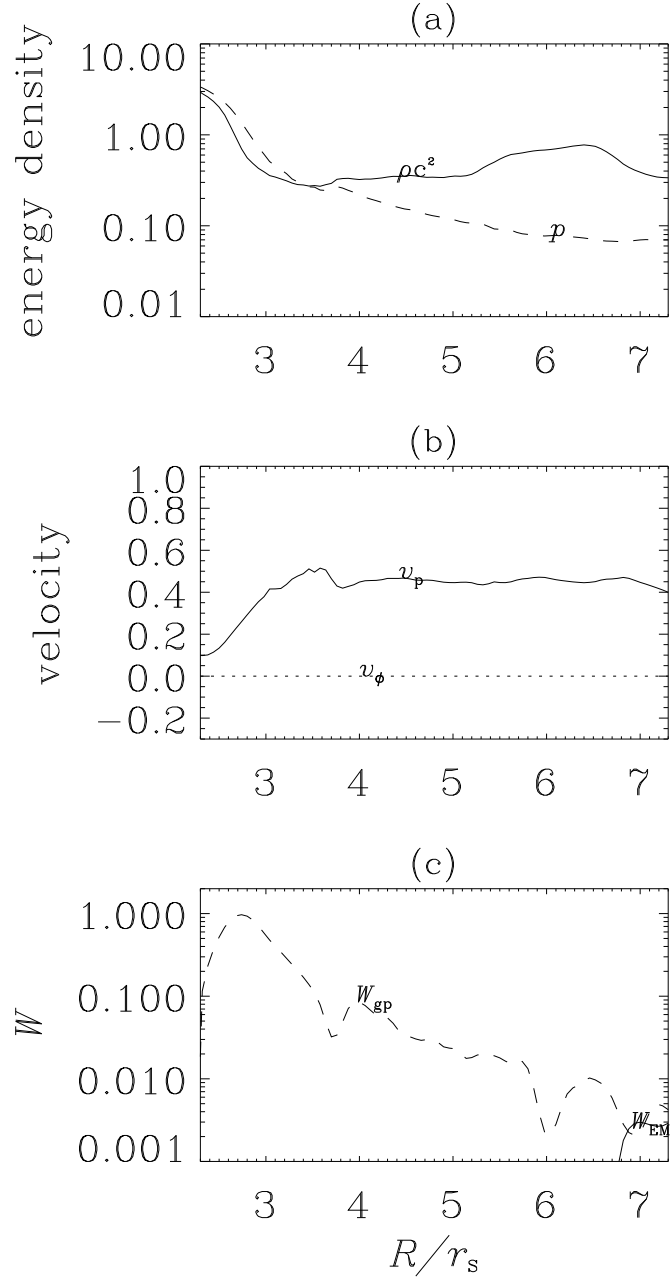


Figure 4: Physical quantities of the Schwarzschild black hole case along $z = R - 2r_s$ ($2.3r_s \leq R \leq 7.3r_s$) at $t = 65\tau_s$ (see straight line in Fig. 2b). (a) Mass density, ρ , gas pressure, p , and poloidal magnetic pressure, $B_\phi^2/2$. (b) Poloidal velocity, v_p and azimuthal velocity, v_ϕ . (c) Power of electromagnetic field (W_{EM}) and gas pressure (W_{gp}) to the acceleration of the jet.

Figure 4 shows the physical variables of the Schwarzschild case at $t = 65\tau_S$ on the line $z = R - 2r_S$ ($2.3r_S \leq R \leq 7.3r_S$). The line is also almost along the main, dense jet (see straight line in Fig. 2b). The terminal velocity of the jet is $0.45c$, sub-relativistic (Fig. 4b). However, the mass density and pressure are relatively high (Fig. 4a). This means that the jet comes from the disk. The jet is accelerated only by gas pressure (Fig. 4c). The high pressure is caused by the shock heating in the disk as the same as in the case of a Keplerian disk around a Schwarzschild black hole [16]. It is reasonable that the azimuthal components of velocity and magnetic field vanish because both the black hole and disk have no rotation. In such a case, magnetic acceleration is not permitted and only a gas pressure driven jet may be formed.

4 Discussion

We have also performed a maximally rotating black hole case ($a = 1$). Preliminary results show that a strong relativistic jet is formed, with a maximum velocity of $0.98c$ (Lorentz factor 5!) and a terminal velocity of $0.9c$ (Lorentz factor, 2.3). Unfortunately, the inner boundary of this calculation is located at $r = 0.8r_S$, which is a little bit far from the horizon, $r_H = 0.5r_S$. We believe that a faster relativistic jet will be formed when we use an inner boundary nearer to the horizon. On the other hand, in the Schwarzschild case with similar initial conditions in the magnetosphere, only a sub-relativistic jet is formed. We have also performed a number of simulations with rotating disks around Schwarzschild black holes [15]. In these cases, all formed jets are sub-relativistic, except for a special case with hydrostatic equilibrium corona [16].

Of course, more simulations of jets formed by rotating black holes accreting magnetized plasma need to be done in order to fully understand this formation mechanism. However, our numerical results show clearly that the spin of the black hole is important in the formation a relativistic jet. A comprehensive model of relativistic jet formation around Kerr black hole, along with more detailed data analysis, will be presented in our following paper.

Recent X-ray observations of black hole candidates (BHCs) in our Galaxy show the relationship between the jet speed and the rotation of the central objects [8]. A quasi-periodic-oscillation (QPO) is found in the power spectrum of the Galactic superluminal source GRO J1655-40 [32] and GRS 1915+105 [33]. Using QPO observations, it is concluded that the both Galactic superluminal sources contain very rapidly rotating black holes ($a \sim 0.95$). Similarly, using the QPOs in Cyg X-1 [34] and in GS 1124-68 [35], it is shown that the black holes in these two sources are spinning less rapidly ($a \sim 0.35$ and $a \sim 0.48$, respectively). Based on these results, Cui, Zhang, & Chen (1998) proposed that the difference between BHCs that are also superluminal jet sources and otherwise *normal* BHCs is in the spin of their black holes. This observational result is consistent with our numerical results.

It is a pleasure to thank K.-I. Nishikawa for suggestions that significantly improved the manuscript. One of author (S. K.) thanks M. Inda-Koide for her discussion and important comments for this study. We also thank M. Takahashi, A. Tomimatsu, J. F. Hawley, R. D. Blandford, M. C. Begelman, P. E. Hardee, J.-I. Sakai, and R. L. Mutel for their discussions and encouragement. We appreciate the support of the National Institute for Fusion Science and the National Astronomical Observatory for the use of super-computers.

References

- [1] J. J. Pearson, *et al.* *Nature* **290** (1981) 365.
- [2] P. A. Hughes, eds., *Beams and Jets in Astrophysics* (Cambridge University Press, New York, 1991).
- [3] M. J. Rees, *Nature* **211** (1966) 468.
- [4] D. Linden-Bell, *Nature* **223** (1969) 690.
- [5] M. J. Rees, *Ann. Rev. Astron. Ap.* **22** (1984) 471.
- [6] I. F. Mirabel & L. F. Rodriguez, *Nature* **371** (1994) 46.
- [7] S. J. Tingay, *et al.* *Nature* **374** (1995) 141.
- [8] W. Cui, S. N. Zhang, & W. Chen, *ApJ* **484** (1998) 383.
- [9] T. Kudoh & K. Shibata, *ApJ* **452** (1995) L41.
- [10] T. Kudoh & K. Shibata, *ApJ* **476** (1997) 632.
- [11] T. Kudoh & K. Shibata, *ApJ* **474** (1997) 362.
- [12] R. Ouyed, R. E. Pudritz, & J. M. Stone, *Nature* **385** (1997) 409.
- [13] D. L. Meier, S. Edgington, P. Godon, D. G. Payne, & K. R. Lind, *Nature* **388** (1997) 350.
- [14] M Livio, K. W. Ogilvie, and J. E. Pringle, *ApJ*, in press.
- [15] S. Koide, K. Shibata, & T. Kudoh, *ApJ*, in press.
- [16] S. Koide, K. Shibata, & T. Kudoh, *ApJ* **495** (1998) L63.
- [17] R. D. Blandford & R. Znajek, *MNRAS* **179** (1977) 433.
- [18] B. Punsly & F. V. Coroniti, *ApJ* **354** (1990) 583.
- [19] M. Takahashi, S. Nitta, Y. Tatematsu, & A. Tomimatsu, *ApJ* **363** (1990) 206.
- [20] M. Takahashi & S. Shibata, *PASJ* **50** (1998) 271.
- [21] K. S. Thorne, R. H. Price, & D. A. Macdonald, *Membrane Paradigm* (Yale University Press, New Haven and London, 1986).
- [22] S. F. Davis, NASA Contractor Rep. 172373, ICASE Rep. No. 84-20 (1984).
- [23] S. Koide, K.-I. Nishikawa, & R. L. Mutel, *ApJ* **463** (1996) L71.
- [24] S. Koide, *ApJ* **478** (1997) 66.
- [25] R. M. Wald, *Phys. Rev. D* **10** (1974) 1680.
- [26] M. Yokosawa, T. Ishizuka, & Y. Yabuki, *PASJ* **43** (1991) 427.
- [27] M. Yokosawa, *PASJ* **45** (1993) 207.
- [28] D. L. Meier, *ApJ*, submitted.
- [29] Y. Uchida & K. Shibata, *PASJ* **37** (1985) 515.
- [30] K. Shibata & Y. Uchida, *PASJ* **38** (1986) 631.
- [31] R. D. Blandford & D. G. Payne, *MNRAS* **199** (1982) 883.
- [32] R. A. Remillard, E. H. Morgan, J. E. McClintock, C. D. Bailyn, A. Oroszek, & J. Greiner, in *Proc. 18th Texas Symp. on Relativistic Astrophysics*, ed. A. Olinto, J. Frieman, & D. Schramm (Singapore: World Scientific Press, 1999) in press.
- [33] E. H. Morgan, R. A. Remillard, & J. Greiner, *ApJ* **482** (1977) 993.
- [34] W. Cui, S. N. Zhang, W. Focke, & J. H. Swank, *MNRAS* **290** (1997) L65.
- [35] T. Belloni, M. van der Klis, W. H. G. Lewin, J. van Paradijs, T. Dotani, K. Mitsuda, & S. Miyamoto, *A & A* **322** (1997) 857.